PHYSICAL REVIEW C VOLUME 26, NUMBER 5 NOVEMBER 1982

Masses of ^{76}Kr and ^{74}Kr

D. M. Moltz and K. S. Toth
Oak Ridge National Laboratory, Oak Ridge, Tennessee 37830

R. E. Tribble, R. E. Neese, and J. P. Sullivan
Cyclotron Institute, Texas A&M University, College Station, Texas 77843

(Received 25 June 1982)

The masses of ^{76}Kr and ^{74}Kr were measured utilizing the ^{78}Kr(^{4}He, ^{6}He) and ^{78}Kr(^{4}He, ^{8}He) reactions. Mass excesses of -68971 ± 13 and -62210 ± 75 keV were obtained for ^{76}Kr and ^{74}Kr, respectively, and found to compare favorably with some mass formulae predictions, but not with others. Speculations about shape differences in light krypton and rubidium isotopes are presented as they relate to various mass formulae.

NUCLEAR REACTIONS ^{4}He+^{78}Kr, $E_{lab}=79.7$ and 102.7 MeV; measured $E_{^{6}He}$, $E_{^{8}He}$; ^{76}Kr, ^{74}Kr deduced Q, masses; magnetic spectrograph. Enriched gas targets.

I. INTRODUCTION

A study of the mass systematics of nuclei far from stability is a sensitive way of comparing nuclear models. It also presents an interesting method for demonstrating specific nuclear phenomena. For instance, model independent two-neutron separation energies (S_{2n}) readily exhibit the standard nuclear shell structure. Sometimes the mass systematics of an $A'=A+4k, T_z=constant$ series of nuclides yields information about nuclei in a particular mass region. One such inference can be made from the $A=4N+1, T_z=+\frac{1}{2}$ series of beta-delayed proton emitters[1-3] as they relate to shape contributions to the nuclear wave functions between the $f_{7/2}$ and $g_{9/2}$ shells. These nuclei are particularly interesting because of the proximity of the proton-drip and $Z=N$ lines.

A recent foray into this region consisted of direct mass measurements[4,5] for most of the known rubidium isotopes. Since that time, we have begun a systematic study[6] of the light neutron-deficient isotopes of rubidium and krypton to determine accurate beta endpoints with an intrinsic germanium detector. (Earlier plastic scintillator measurements have been found to be in error, requiring masses obtained in this manner to be reexamined; the analysis technique used in Ref. 6 has been described[7-9] elsewhere.) Nearer the valley of stability, however, many unstable proton-rich nuclei decay only by electron capture. In some of these instances transfer reactions may be utilized to measure nuclear masses. One such pivotal nucleus with a low Q_β value whose mass had not been measured is ^{76}Kr. We therefore undertook to determine its mass excess by using the ^{78}Kr(^{4}He,^{6}He) reaction. As part of the study we also utilized the ^{78}Kr(^{4}He,^{8}He) reaction to measure the mass of ^{74}Kr; its decay energy to ^{74}Br is known[10] to ±120 keV. Since the start of our investigation, the mass of ^{76}Kr was measured[11] via the ^{78}Kr(p,t) reaction.

II. EXPERIMENTAL PROCEDURE

The mass of ^{76}Kr was determined by measuring the Q value for the ^{78}Kr(^{4}He,^{6}He)^{76}Kr reaction at $E_{^{4}He}=79.7$ MeV; the mass of ^{74}Kr was then measured via the ^{78}Kr(^{4}He,^{8}He)^{74}Kr reaction at $E_{^{4}He}=102.7$ MeV, an incident energy chosen to permit simultaneous observation of ^{6}He and ^{8}He particles leading to the ground states of ^{76}Kr and ^{74}Kr. Alpha-particle beams from the Texas A&M University 224-cm cyclotron were incident upon enriched krypton targets (90+% ^{80}Kr and 99 +% ^{78}Kr) maintained in a gas cell statically pressurized to 40–60 Torr at 300 K. This ~100 cm^3 gas cell was isolated from the surrounding vacuum by ~1.9 mg/cm^2 Havar foil. The well-collimated reaction products were detected on the focal plane

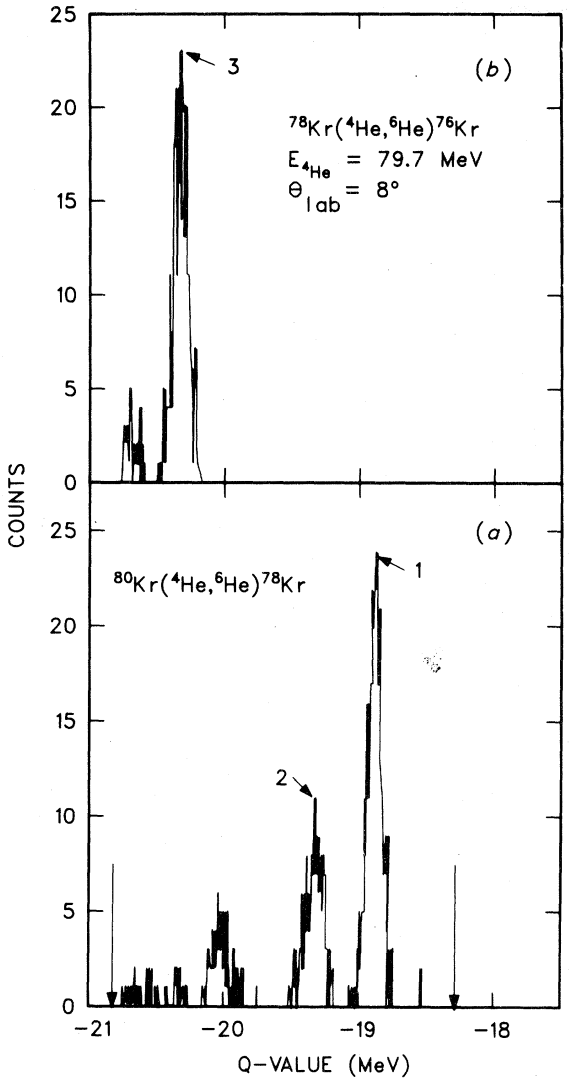

FIG. 1. Gated ^{6}He position spectra at $E_{^4He}$=79.7 MeV for the reactions: (a) ^{80}Kr(^{4}He,^{6}He)^{78}Kr and (b) ^{78}Kr(^{4}He,^{6}He)^{76}Kr. Large arrows indicate detector limits. Peaks labeled by numerals correspond to: (1) ^{78}Kr ground state, (2) first 2^+ excited state in ^{78}Kr, and (3) ^{76}Kr ground state.

of an Enge split-pole magnetic spectrograph by a 10-cm single-wire gas proportional counter, used as a ΔE detector, with a 5.0×1.0 cm×600 μm solid state silicon detector serving as an E detector. The time-of-flight (TOF) of the particles through the spectrograph [relative to the cyclotron radio frequency (rf)] and the particle position obtained via charge division in the gas counter were stored in addition to the E and ΔE signals in event-by-event mode on magnetic tape for subsequent playback. Figure 1 shows a typical position spectrum gated by suitable bounds for ^{6}He particles in the E, ΔE, and TOF spectra. This experimental setup has been shown[12] to reject spurious background events at a level below 200 pb/(sr MeV) for medium mass targets. Additional experimental details may be found elsewhere.[13–15]

While the experiment consisted of two distinct mass measurements, several parameters remained unchanged throughout. Elastically-scattered 79.7-MeV $^{4}He^{2+}$ particles were used to determine the vertical efficiency of 0.82. The spectrograph was placed at $\theta_{lab}=8°$ with an entrance aperture corresponding to 2.6 msr. The laboratory angle was chosen after comparison with the ^{8}He angular distribution[16] arising from the ^{64}Ni(^{4}He,^{8}He)^{60}Ni reaction. A 0.2-mm Kapton absorber foil was placed between the gas proportional counter and the silicon detector to ensure that the ^{8}He particles would stop in the silicon counter. After initially charging the gas cell with 40 Torr of ^{80}Kr, calibration of the position spectrum was accomplished by varying the spectrograph magnetic field setting to change the position of the ^{6}He particles associated with the ground state of ^{78}Kr. Figure 1(a) represents the final ^{6}He spectrum arising from ^{80}Kr. The ^{80}Kr gas was then removed and was replaced with 40 Torr of ^{78}Kr gas resulting in the spectrum shown in Fig. 1(b). All spectra were collected in short runs corresponding to an average beam intensity of $\sim$1.0 μA and an integrated beam of 2.5 mC.

The ^{4}He beam energy was then raised to 102.7 MeV and the ^{78}Kr target pressure to 60 Torr. The rest of the experiment was conducted under these conditions. The integrated beam for this second part was 74.7 mC at an average beam intensity of $\sim$1.2 μA. On-line data sorting was employed to record the ^{6}He rate as a monitor of the relative stability of all experimental systems.

III. RESULTS AND COMPARISONS

The ^{6}He position spectrum arising from the ^{80}Kr(^{4}He,^{6}He)^{78}Kr reaction is shown at the bottom of Fig. 1, while the top portion of this figure corresponds to a ^{6}He spectrum due to the ^{78}Kr(^{4}He,^{6}He)^{76}Kr reaction obtained with the same cyclotron and spectrograph parameters. The measured Q value of -20.351 MeV yields a mass excess of -68971 ± 13 keV for ^{76}Kr. The 13-keV uncertainty arises from a centroid and calibration uncertainty of 10 keV added in quadrature to the 8-keV uncertainty[17] in the ^{78}Kr mass excess. The 324 integrated peak events in Fig. 1 correspond to a laboratory cross section of 6 ± 2 μb/sr for the ground

state of ^{76}Kr averaged over the 2.6 msr solid angle centered at $\theta_{lab}=8°$. The width in the observed peak is due primarily to energy straggling in the gas target and the Havar isolation foil.

Raising the bombardment energy to 102.7 MeV insured the simultaneous observation of ^{6}He and ^{8}He particles at the detector location on the focal plane. Although the ^{6}He position spectrum could provide a convenient system check, the primary source of background in the ^{8}He spectrum came from ^{7}Li events. These ^{7}Li particles exhibit almost identical E and TOF spectra to those of ^{8}He, but $\Delta E_{^{7}\mathrm{Li}} \simeq 2\Delta E_{^{8}\mathrm{He}}$, permitting an effective separation and identification. A two-dimensional plot of E vs TOF is shown in Fig. 2. The ΔE gate used here was set by observing a null effect upon the ^{4}He^{+} peak. (^{4}He^{+} and ^{8}He^{2+} have the same dE/dx.) The ^{8}He peak remained intact while the ^{7}Li peak decreased by a factor of 50 from the ungated spectrum. The ^{8}He gated position spectrum is shown in Fig. 3. The four integrated counts correspond to a laboratory cross section of 1.4 ± 0.8 nb/sr at $\theta_{lab}=8°$.

The Q value for the ^{78}Kr(^{4}He,^{8}He) reaction was found to be -41.12 MeV which yields a mass excess of -62210 ± 75 keV for ^{74}Kr. The 75-keV uncertainty was calculated from a 70-keV peak-centroid and calibration uncertainty and a 30-keV beam energy uncertainty. This latter value is estimated from past measurements with the analyzing magnet contained within the cyclotron beam optics system. Since this value contributes very little to the final error, a direct beam energy measurement was deemed unnecessary. The one higher energy event is consistent with the background observed with a 99+% ^{20}Ne target used with this gas cell in a new measurement[18] of the mass of the unbound nuclide ^{16}Ne via the ^{20}Ne(^{4}He,^{8}He)^{16}Ne reaction.

Our value of -68971 ± 13 keV for the mass excess of ^{76}Kr agrees well with a recent[11] value obtained from the ^{78}Kr$(p,t)^{76}$Kr reaction of -68968 ± 15 keV. This excellent agreement permits us to adopt a value of -68970 ± 11 keV for the ^{76}Kr mass excess. The measured cross section for this latter reaction is approximately two orders of magnitude larger than that for the (^{4}He,^{6}He) reaction. This large discrepancy is somewhat surprising because in principle these reactions may proceed via three differing mechanisms[19]: direct two-neutron transfer, indirect multistep two-neutron transfer, and two sequential one-neutron transfers. The sequential transfer might seemingly be more important for the (^{4}He,^{6}He) reaction than for the (p,t) case because of the greater similarity between the ^{5}He and ^{6}He wave functions than for the deuteron and triton wave functions. Jang and Sorensen[19] conclude that this sequential transfer is not negligible for the (^{4}He,^{6}He) reaction. However, the direct process would tend to favor the enhanced cross section for the (p,t) reaction over the (^{4}He,^{6}He) reaction, possibly indicating the dominance of the direct channel in this mass region, an idea which has been previously espoused.[20] The cross section for the (^{4}He,^{8}He) reaction (1.4 ± 0.8 nb/sr) is consistent with other results[16] in this region. Additionally, the ratio $(d\sigma/d\Omega)_{^{8}\mathrm{He}}/(d\sigma/d\Omega)_{^{6}\mathrm{He}}$ is not extraordinary.

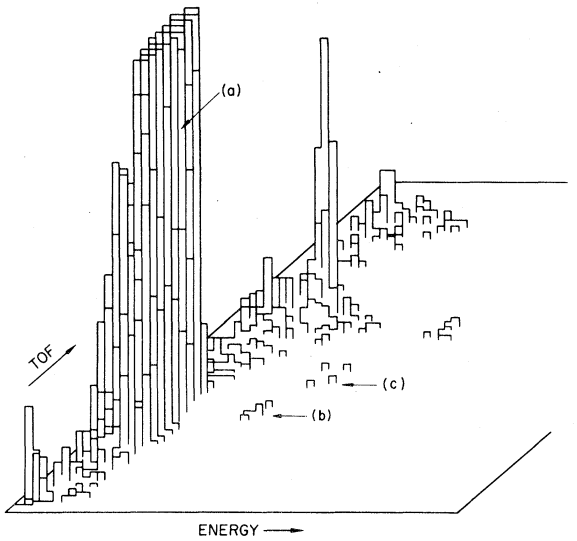

FIG. 2. Two-dimensional plot of energy (abscissa) vs TOF (ordinate) with a ^{4}He^{+} ΔE gate. Labeled peaks correspond to: (a) ^{4}He^{+}, (b) ^{8}He^{2+}, and (c) ^{7}Li^{2+}.

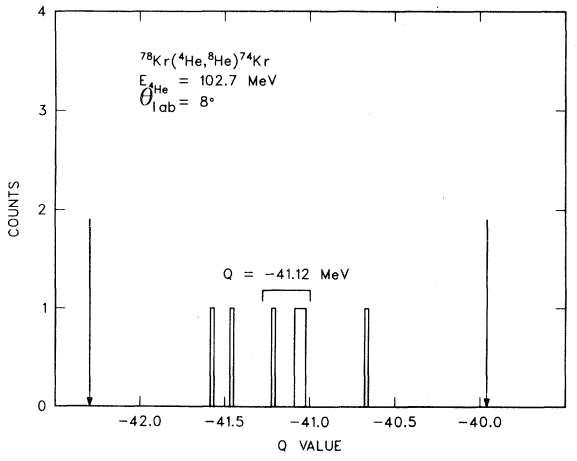

FIG. 3. Gated ^{8}He position spectrum at $E_{^{4}\mathrm{He}}=102.7$ MeV for the ^{78}Kr(^{4}He,^{8}He)^{74}Kr reaction. Arrows indicate detector limits.

Since evidence for a similar direct process for the four-neutron transfer in the (^{4}He,^{8}He) reaction has been presented[16] elsewhere, this could further be interpreted as evidence (albeit indirect) for the notion of a primarily direct process in the (^{4}He,^{6}He) reaction.

The mass excess of -62210 ± 75 keV for ^{74}Kr disagrees with the accepted value[17] of -62020 ± 100 keV based upon a Q_β mass difference measurement[10] utilizing a plastic scintillator beta spectrometer. Since the mass of ^{74}Br (-65295 ± 15 keV) was determined accurately by a (p,n) threshold reaction,[21] this difference probably originates with an incorrect level structure for ^{74}Br or the inherently bad energy resolution of the plastic scintillator system. These two problems are not uncommon in beta endpoint measurements (see, e.g., Ref. 6). We therefore adopt our value of -62210 ± 75 keV for the mass excess of ^{74}Kr. The relative importance of these adjustments to the mass excess values and their uncertainties will be discussed in terms of the overall mass surface in the next section.

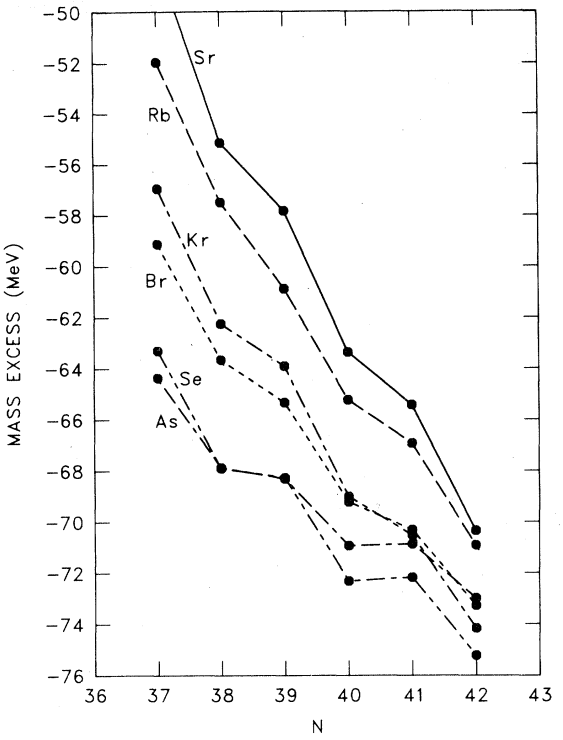

FIG. 4. Mass excesses plotted vs neutron number for nuclei with $Z=33-38$ and $N=37-42$.

IV. DISCUSSIONS AND CONCLUSIONS

It is often necessary to view a particular set of mass measurements as part of a larger systematic picture. This approach, adopted for the remainder of the discussion, is particularly useful in delineating regions of deformation such as that found in the neutron deficient krypton, rubidium, and strontium nuclei. Table I lists the updated mass excess values for nuclei with ($Z=33-38$, $N=37-42$) while Fig. 4 graphically depicts this same region. Many mass

TABLE I. Partial tabulation of updated mass excesses in keV. Uncertainties are enclosed in parentheses. Numbers given in the lower line represent calculations made in this investigation using the transverse Garvey-Kelson relationship (see text). Values have been taken from Ref. 17 unless otherwise noted.

Z	$N=37$	38	39	40	41	42
38(Sr)			−57830(210)[a,b]		−65600(130)[c]	
	−47950(460)	−55165(250)	−58869(135)	−63360(115)	−65400(85)	−70395(75)
37(Rb)	−51984(270)[d]	−57491(188)[d]	−60906(45)[e]	−65209(50)[e]	−66908(22)[f]	−70902(42)[d]
	−52156(240)	−58010(100)	−59789(100)	−64666(70)		
36(Kr)	−56980(140)	−62210(75)[a]		−68970(11)[a,g]	−70481(43)[e]	−74150(8)
	−56400(90)	−62455(60)	−63917(17)	−69489(50)	−70342(20)	
35(Br)		−63670(220)	−65295(15)	−69159(20)	−70303(15)	−73241.5(38)
	−59169(35)	−63693(21)				
34(Se)		−67894(12)	−68209(11)	−72212.7(26)	−72169.0(24)	−75259.2(25)
	−63346(25)					
33(As)	−64339(20)	−67893(4)	−68232(7)	−70949(4)	−70859.7(25)	−73033.9(23)

[a]This work.
[b]Reference 1.
[c]Reference 22.
[d]Reference 5.
[e]Reference 6.
[f]Reference 23.
[g]Reference 11.

prediction formulae use known mass excesses to obtain a series of parameters for semiempirical calculations. Unfortunately, these parameters might dramatically change with new input masses. The Garvey-Kelson[24,25] mass relationship may be used in either this latter way or in a recursive building sense. The transverse form of this equation for neutron-deficient nuclei, written as

$$M(A,T_Z)\simeq M(A,T_Z+2) +M(A+1,T_Z+\tfrac{1}{2})-M(A+1,T_Z+\tfrac{3}{2}) +M(A-1,T_Z+\tfrac{1}{2})-M(A-1,T_Z+\tfrac{3}{2}) , \quad (1)$$

can be solved as a partial differential equation for $M(A,T_Z)$. (This approach is utilized by Jänecke.[26]) Another approach utilizes the recursive nature of the formula to build newer predictions further from stability. This method of course requires good input masses to yield reliable mass predictions. The second (or lower) entry for many of the nuclei listed in Table I is the continued reapplication of this relationship. Quoted uncertainties represent only the accumulated errors from input values.

One of the most instructive and informative ways to view new mass values on the nuclidic mass surface is through comparisons with differing theoretical models, including the revised Garvey-Kelson method delineated earlier. Table II lists predictions from several models and the differences between them and the masses obtained in this work and other recent results[6] in this region. Myers's droplet model[27] consistently overpredicts the stability of these masses, as is indicated by the similarity of the average ($\langle\Delta\rangle$) and the root-mean-square average ($\Delta_{\rm rms}$). This case may be contrasted with the revised Garvey-Kelson predictions where $|\langle\Delta\rangle| \neq |\Delta_{\rm rms}|$. This situation is predicated upon the ^{77}Sr case which requires the mass of ^{76}Rb (a mass which only Groote *et al.*[27] predict with even relative success). Thus, all of the Garvey-Kelson based predictions give similar results. Particular attention should be given to the excellent agreement between the experimental ^{76}Kr mass and the prediction of Möller and Nix.[28] The primary idea behind their calculations[29] incorporates shape independent and dependent effects and requires the empirical determination of only five constants by fitting known masses. Thus, one might expect that the nuclidic mass surface calculated in this manner would be sensitive to any shape changes. The mass of any predicted deformed nuclei would provide some small test for this hypothesis. The predicted onset of prolate deformation in the krypton isotopes is at ^{76}Kr. Unfortunately, this deformation onset in the rubidium

TABLE II. Experimental mass excesses (in MeV) for ^{74}Kr, ^{76,77}Kr, ^{76,77}Rb, and ^{77}Sr compared with predictions from various mass models.

Isotope	Experimental mass	Revised Garvey-Kelson	Jänecke[a] Garvey-Kelson	Möller[b] and Nix	Myers[a]	Liran[a] and Zeldes	Comay[a] and Kelson	Groote, Hilf,[a] and Takahashi
^{74}Kr	−62.210(75)	−62.46	−62.32	−62.09	−64.04	−62.20	−62.45	−62.66
^{76}Kr	−68.970(11)	−69.49	−69.07	−68.98	−70.22	−68.91	−69.16	−68.89
^{77}Kr	−70.481(43)[c]	−70.34	−70.12	−69.58	−71.35	−69.80	−70.19	−70.26
^{76}Rb	−60.906(45)[c]	−59.79	−59.98	−60.23	−62.05	−59.21	−59.94	−60.66
^{77}Rb	−65.209(50)[c]	−64.77	−64.91	−65.04	−66.54	−64.12	−64.91	−65.25
^{77}Sr	−57.830(210)[d]	−58.87	−57.30	−57.77	−59.67	−56.21	−57.53	−58.14
				Difference (experiment minus theory)				
^{74}Kr		0.25	0.11	−0.12	1.83	0.01	0.24	0.45
^{76}Kr		0.52	0.10	0.01	1.25	−0.06	0.19	−0.08
^{77}Kr		−0.14	−0.36	−0.90	0.87	−0.68	−0.29	−0.22
^{76}Rb		−1.12	−0.93	−0.68	1.14	−1.70	−0.97	−0.25
^{77}Rb		−0.44	−0.30	−0.17	1.33	−1.09	−0.30	−0.04
^{77}Sr		1.04	−0.53	−0.06	1.84	−1.62	−0.30	−0.31
	$\langle\Delta\rangle$:	0.02	−0.32	−0.32	1.38	−0.86	−0.24	0.04
	$\Delta_{\rm rms}$:	0.69	0.48	0.47	1.42	1.09	0.47	0.26

[a]Reference 27.
[b]Reference 28.
[c]Reference 6.
[d]Reference 1 and this work.

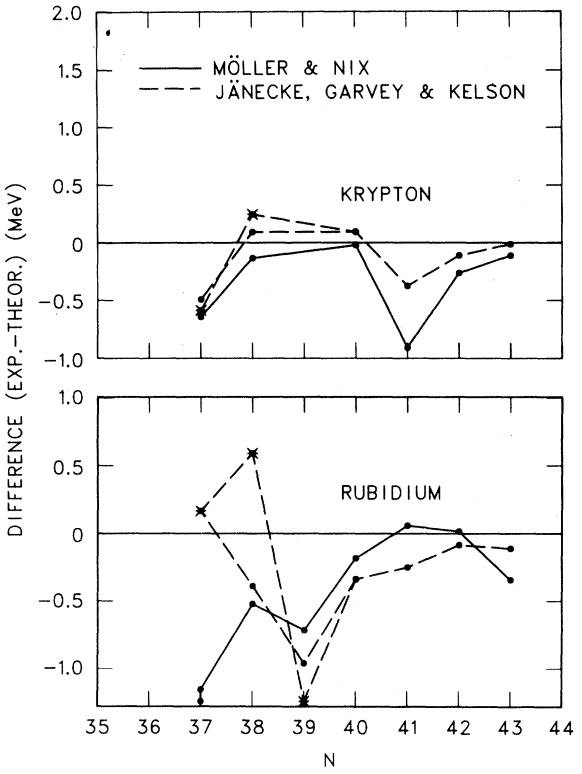

FIG. 5. Mass formulae comparisons for krypton and rubidium isotopes with $N=37-43$. Points marked with an $\times$ indicate values obtained via the revised Garvey-Kelson method given in the text.

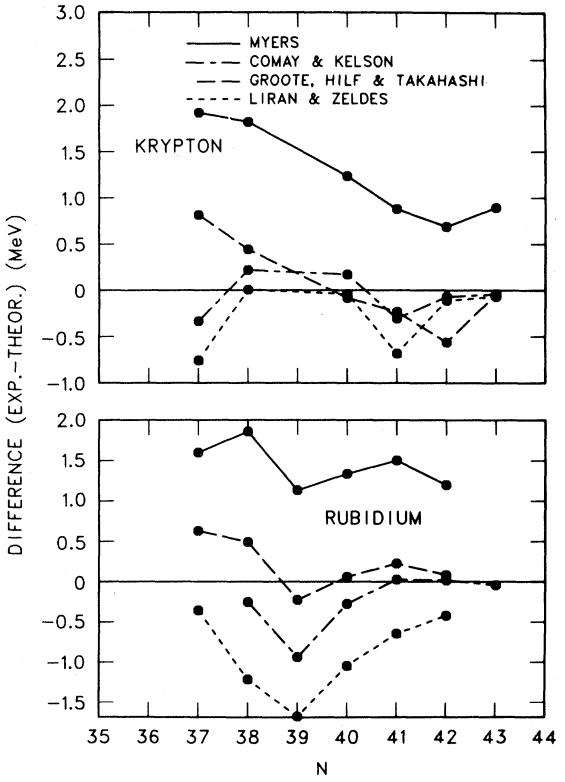

FIG. 6. Mass formulae comparisons for krypton and rubidium isotopes with $N=37-43$. All values are taken from Ref. 27.

isotopes occurs around $A\sim80$, a member of the original ensemble of averaged masses. A systematic study of the strontium mass excesses would therefore be of great value for comparison.

Figures 5 and 6 show graphical representations of the differences between the experimental masses and several theoretical predictions for the krypton and rubidium isotopes. Generally, all of the predictions incorrectly give the mass of ^{76}Rb. Although the value of Groote *et al.*[27] is not terribly different, a definite trend reversal is evident. If there exists some quasimagic number around $N=39$ in these deformed nuclei, then the mass of ^{75}Kr must be obtained in addition to improving the error bar for ^{77}Sr. Two-neutron separation energies in this region could be interpreted as supporting this claim; however, error bars on several entries are far too large to generalize in this manner. The mass of ^{75}Kr should also provide an additional clue in the even-Z neutron pairing energy theoretical gap. Although the Möller-Nix formula seems to handle unpaired protons as a function of shape relatively well, a systematic underprediction of the neutron pairing energy seems evident in the krypton isotopes. A systematic study of the strontium masses would help test this hypothesis. The special case of the self-conjugate nucleus, ^{76}Sr, would permit testing of the Wigner energy terms in various mass models. Thus, even though the present study adds two pieces to the nuclidic mass surface between the $f_{7/2}$ and $g_{9/2}$ shells, it is clear that remeasurements and new values must be obtained. These mass data can then be combined with nuclear structure information to also provide tests for the degree of shape changes in this portion of the chart of the nuclides.

ACKNOWLEDGMENTS

We wish to thank Ms. C. J. Woodward for her assistance with the data analysis. Oak Ridge National Laboratory is operated by Union Carbide Corporation for the U. S. Department of Energy under Contract No. W-7405-eng-26. The work at Texas A & M was also supported in part by the U. S. Department of Energy and the R. A. Welch Foundation.

[1]J. C. Hardy, J. A. Macdonald, H. Schmeing, T. Faestermann, H. R. Andrews, J. S. Geiger, R. L. Graham, and K. P. Jackson, Phys. Lett. 63B, 27 (1976).
[2]J. A. Macdonald, J. C. Hardy, H. Schmeing, T. Faestermann, H. R. Andrews, J. S. Geiger, R. L. Graham, and K. P. Jackson, Nucl. Phys. A288, 1 (1977).
[3]J. C. Hardy, T. Faestermann, H. Schmeing, J. A. Macdonald, H. R. Andrews, J. S. Geiger, R. L. Graham, and K. P. Jackson, Nucl. Phys. A371, 349 (1981).
[4]M. Epherre, G. Audi, C. Thibault, R. Klapisch, G. Huber, F. Touchard, and H. Wollnik, Phys. Rev. C 19, 1504 (1979).
[5]G. Audi, M. Epherre, C. Thibault, A. H. Wapstra, and K. Bos, Nucl. Phys. A378, 443 (1982).
[6]D. M. Moltz, K. S. Toth, F. T. Avignone, III, H. Noma, B. G. Ritchie, and B. D. Kern, Phys. Lett. 113B, 16 (1982).
[7]T. A. Girard and F. T. Avignone, III, Nucl. Instrum. Methods 154, 199 (1978).
[8]F. T. Avignone, III, L. P. Hopkins, and Z. D. Greenwood, Nucl. Sci. Eng. 72, 216 (1979).
[9]F. T. Avignone, III, H. Noma, D. M. Moltz, and K. S. Toth, Nucl. Instrum. Methods 189, 453 (1981).
[10]H. Schmeing, J. C. Hardy, R. L. Graham, and J. S. Geiger, Nucl. Phys. A242, 232 (1975).
[11]S. Matuski, N. Sakamoto, K. Ogino, Y. Kadota, T. Tanabe, and Y. Okuna, Nucl. Phys. A370, 1 (1981).
[12]R. E. Tribble, J. D. Cossairt, D. P. May, and R. A. Kenefick, Phys. Rev. C 16, 917 (1977).
[13]R. E. Tribble, R. A. Kenefick, and R. L. Spross, Phys. Rev. C 13, 50 (1976).
[14]R. E. Tribble, J. D. Cossairt, and R. A. Kenefick, Phys. Lett. 61B, 353 (1976).
[15]R. E. Tribble, D. M. Tanner, and A. F. Zeller, Phys. Rev. C 22, 17 (1980).
[16]R. E. Tribble, J. D. Cossairt, K-I. Kubo, and D. P. May, Phys. Rev. Lett. 40, 13 (1978).
[17]A. H. Wapstra and K. Bos, At. Data Nucl. Data Tables 19, 175 (1977).
[18]R. E. Tribble *et al.* (unpublished).
[19]S. Jang and B. Sørensen, Nucl. Phys. A344, 315 (1980).
[20]M. Hamm, C. W. Towsley, R. Hanus, K. G. Nair, and K. Nagatani, Phys. Rev. Lett. 36, 846 (1976).
[21]D. H. Lueders, J. M. Daley, S. G. Buccino, F. E. Durham, C. E. Hollandsworth, W. P. Bucher, and H. D. Jones, Phys. Rev. C 11, 1470 (1975).
[22]C. J. Lister, P. E. Haustein, D. E. Alburger, and J. W. Olness, Phys. Rev. C 24, 260 (1981).
[23]G. K. Bavaria, J. E. Crawford, S. Calamawy, and J. E. Kitching, Z. Phys. A 302, 329 (1981).
[24]G. T. Garvey and I. Kelson, Phys. Rev. Lett. 16, 197 (1966).
[25]G. T. Garvey, W. J. Gerace, R. L. Jaffe, I. Talmi, and I. Kelson, Rev. Mod. Phys. 41, S1 (1969).
[26]J. Jänecke, At. Data Nucl. Data Tables 17, 455 (1976).
[27]S. Maripuu and K. Way, At. Data Nucl. Data Tables 17, 410 (1976).
[28]P. Möller and J. R. Nix, At. Data Nucl. Data Tables 26, 165 (1981).
[29]P. Möller and J. R. Nix, Nucl. Phys. A361, 117 (1981).